American Mineralogist, Volume 75, pages 791–800, 1990

Factors influencing short-lived blue cathodoluminescence of α-quartz

KARL RAMSEYER
Geologisches Institut, Universität Bern, 3012 Bern, Switzerland
JOSEF MULLIS
Mineralogisch-Petrographisches Institut, Universität Basel, 4056 Basel, Switzerland

ABSTRACT

Crystals of α-quartz from fissures in the Swiss Alps and from the island of Grand Canary were investigated to determine the factors influencing their cathodoluminescence characteristics.

The cathodoluminescence of α-quartz is commonly a short-lived blue, blue-green, or yellow color with nonluminescent areas. Long-lived violet and a brown luminescence of increasing intensity are uncommon for α-quartz.

Cathodoluminescence observations, fluid-inclusion studies, microprobe analysis, heat- and electrodiffusion treatments and morphological data revealed that the cathodoluminescence of α-quartz is influenced by the uptake of charge balancing single charged cations associated with the substitution of Al for silica. Electrodiffusion studies indicate that H can cause short-lived cathodoluminescence. The amount and distribution of the trace elements in α-quartz are controlled by the growth dynamics, growth direction, twinning, fracturing, and natural α- or γ-irradiation.

Physicochemical growth parameters, such as crystallization temperature, pressure, composition, and concentrations of volatiles in crystallizing fluids, do not influence the short-lived cathodoluminescence of α-quartz.

INTRODUCTION

Electron-excited luminescence, or cathodoluminescence, in naturally grown α-quartz was first reported by Goldstein (1907). Later, Smith and Stenstrom (1965), Long and Agrell (1965), Sippel (1968), Sprunt et al. (1978), Zinkernagel (1978), and Matter and Ramseyer (1985) demonstrated the ability of this technique to distinguish α-quartz precipitated from an aqueous chloride solution (i.e, diagenetic or hydrothermal origin) from quartz crystallized in a melt (i.e., igneous or metamorphic origin).

Few data exist on the cathodoluminescence behavior of diagenetic or hydrothermally formed α-quartz, which has generally been thought to be nonluminescent (Sippel, 1965; Smith and Stenstrom, 1965; Zinkernagel, 1978) or to possess nondetectable short-lived luminescence (Zinkernagel, 1978). Improvements in the detection limits of very faint luminescence intensities by a new type of cathodoluminescence microscope enabled Ramseyer et al. (1988) to record a variety of short-lived luminescence colors in α-quartz precipitated from an aqueous chloride solution.

The purpose of this paper is to determine crystallographic, physical, and chemical parameters that influence the cathodoluminescence of diagenetically or hydrothermally formed α-quartz. More than 75 quartz crystals from nine localities in the Swiss Alps (Mullis, 1975, 1976, 1980, 1982), from cavities in a Miocene basalt (Canary Islands; Mullis and Sigl, 1982) and a quartz crystal used in electrodiffusion experiments (kindly provided by the Mineralogisches Institut ETH-Zürich) were selected to cover the physicochemical conditions present in natural diagenetic and hydrothermal systems (Table 1) and to assess the consistency of cathodoluminescence distributions.

METHODS

An improved cathodoluminescence microscope (Ramseyer et al., 1989) was used to examine the faint and short-lived luminescence colors in fissure quartz. The applied beam current density for the cathodoluminescence was 0.2–0.4 $\mu A/mm^2$ at 30 keV electron energy. Luminescence characteristics were recorded on Ektachrome 400 color slide film with 1¾-minutes exposure time and developed at 800 ASA. Changes in the luminescence during electron bombardment due to the relatively long exposure time (Ramseyer et al., 1989) dictate that comparable results can only be obtained by using identical operating conditions and areas of no previous electron bombardment. When these requirements are fulfilled, then the consistency of results obtained is excellent. Since lengthy electron bombardment leads to modification of the emission spectra, cathodoluminescence characteristics are compared by means of qualitative observations of previously unbombarded areas on color slides. The photographic results obtained are therefore a time-integrated function of the continuously changing luminescence characteristics. The luminescence spectra were also recorded

0003–004X/90/0708–0791$02.00

Table 1. Morphology and physicochemical parameters calculated from phase transitions in fluid inclusions

Locality	Morphology	Twinning	Color	Salinity (mol%)	Fluid type	Temperature (°C)	Pressure (MPa)	Growth mode
Grand Canary	scepter	Brazil	clear	0.5	I	≈150	≈0.5	rapid discont.
Blattenberg	scepter	Brazil	clear	?	II	≈150	<100	rapid discont.
Val d'Illiez	prismatic	Brazil	clear	0.6	III	200–220	140–180	slow discont.
	scepter	Brazil	clear	?	IV	180–200	44–47	rapid discont.
Brunnital	prismatic	Brazil	clear	0.5	V	280–300	220–270	slow discont.
Windgällen	prismatic	Brazil	clear	1.3	V	300	210	slow discont.
Gigerwald	prismatic	Brazil	clear	2.1	V	300	170	slow discont.
Amethystkehle	prismatic	Dauphinée	brown	1.9	V	400–420	320–360	slow cont. + discont.
	scepter	Brazil	violet	0.3	VII	260–300	46–65	rapid discont.
Val Giuv	prismatic	Dauphinée	brown	2.5	V	400–420	300–340	slow cont. + discont.
	scepter	Brazil	violet	?	VII	240–280	190–210	rapid discont.
Grosstal	prismatic	Dauphinée	clear	1.3	V	380–400	240–280	slow cont.
Camperio	prismatic	Dauphinée	clear	1.2	VI	420–450	220–250	slow cont. + discont.
	scepter	Brazil	clear	?	VII	320–340	34–39	rapid discont.

Note: I = steam; II = >80 mol% CH_4 + 5–15 mol% higher hydrocarbons; III = >94 mol% H_2O + 1–2 mol% CH_4 + <1 mol% higher hydrocarbons; IV = >80 mol% CH_4 + <1 mol% higher hydrocarbons; V = >94 mol% H_2O + <1 mol% CH_4, higher hydrocarbons; VI = >80 mol% H_2O + 10–20 mol% CO_2; VII = >40 mol% CO_2

at a speed of 5 nm per s on a SPEX Minimate monochromator equipped with a R446 Hamamatsu photomultiplier. Entrance and exit slits of the monochromator were set for an effective resolution of 10 nm. The measured spectra were corrected for the spectral response of the recording system between 350 and 730 nm.

Selected samples were subjected to artificial γ-irradiation by a cobalt-60 source (5×10^7 rad, Mullis, 1976), electron bombardment, and 1 to 500 h of heat treatment (between 110 and 700 °C with an uncertainty of ±50 °C) prior to their examination.

A Chaixmeca heating and freezing stage (Poty et al., 1976) attached to a petrographic microscope was used to study phase transitions (Roedder, 1984; Mullis, 1987) in fluid inclusions. Temperatures were measured using the technique of Poty et al. (1976). Contents of higher hydrocarbons (HHC, C > 1), and of CH_4, CO_2 and N_2 in fluid inclusions were additionally determined by mass spectrometry and Raman spectroscopy (Dhamelincourt et al., 1979). Bulk fluid compositions were calculated after the technique of Mullis (1979, 1987) and Ramboz et al. (1985). Approximate trapping pressures were estimated using the *PVT* data for the systems H_2O-NaCl, H_2O-CO_2-NaCl, H_2O-CO_2-CH_4 and CO_2-N_2 (Potter and Brown, 1977; Bowers and Helgeson, 1983; Jacobs and Kerrick, 1981; Holloway, 1981).

The Al content of quartz was measured using an ARL-SEMQ electron microprobe with a wavelength dispersive system (TAP-crystal) at 20-nA sample current, 15-keV electron energy and 100-s counting time. The detection limit (3σ-error) for Al in quartz was found to be 50 ppm.

Results

The most common cathodoluminescence colors in the α-quartz examined on color slides are different shades of short-lived blue and blue-green (Figs. 1, 2). Violet (Figs. 3B, 2H), yellow (Figs. 3A, 2B) and brown (Figs. 3B, 2H)

→

Fig. 1. Scale bar is 500 μm. (**A**) Fissure quartz from Grand Canary, with cut surface perpendicular to the *c* axis. Originally this crystal was mostly nonluminescent; however, after 2 min of continuous electron bombardment, brown lamellae reflecting the growth pattern appeared. A growth pattern (arrows), which encircles the center hole, is partly visible through brown luminescing growth zones. (**B**) Fissure quartz from Blattenberg with a scepter morphology, cut parallel to the *c* axis. This largely nonluminescent crystal exhibits dark blue luminescence only at the junctions of rhombohedral and prismatic growth faces. (**C**) Fissure quartz from Val d'Illiez with a prismatic core (P) and scepter overgrowth (S), cut parallel to the *c* axis. The scepter part exhibits a complex luminescence distribution, with zonation parallel to the prism (m) and the positive (r) and the negative (z) rhombohedra. (**D**) Fissure quartz from Val d'Illiez with scepter morphology, with cut surface normal to the *c* axis. The zoned luminescence of the growth normal to the prism faces (yellowish color) is overprinted by the occurrence of Brazil twinning (blue areas). (**E**) Artificially γ-irradiated fissure quartz from Val d'Illiez, cut parallel to the *c* axis and viewed in transmitted light. The crystal exhibits smoky zones, which correlate with the luminescence growth pattern of Figure 1F. (**F**) Same crystal as in Figure 1E, but exhibiting cathodoluminescence. All parts that show pronounced coloration by γ-irradiation are nonluminescent. This crystal is less luminescent than the crystal shown in Figure 1C, particularly in its prismatic core (P). Only the intermediate discontinuous slowly grown zone (I) is not strongly affected by γ-irradiation. The numbers refer to the location of the microprobe analyses from Table 2. (**G**) Artificially γ-irradiated fissure quartz from Windgällen, cut parallel to the *c* axis, in transmitted light. The visible zonation in this crystal is characteristic of slow discontinuous growth normal to the positive and negative rhombohedra. (**H**) Same crystal as shown in Figure 1G, but exhibiting luminescence. The darker luminescing growth bands correspond with the more intensely colored, smoky zones of Figure 1G. Microprobe analysis indicates that the two dark blue luminescing zones (arrows) contain more than 300 ppm of Al.

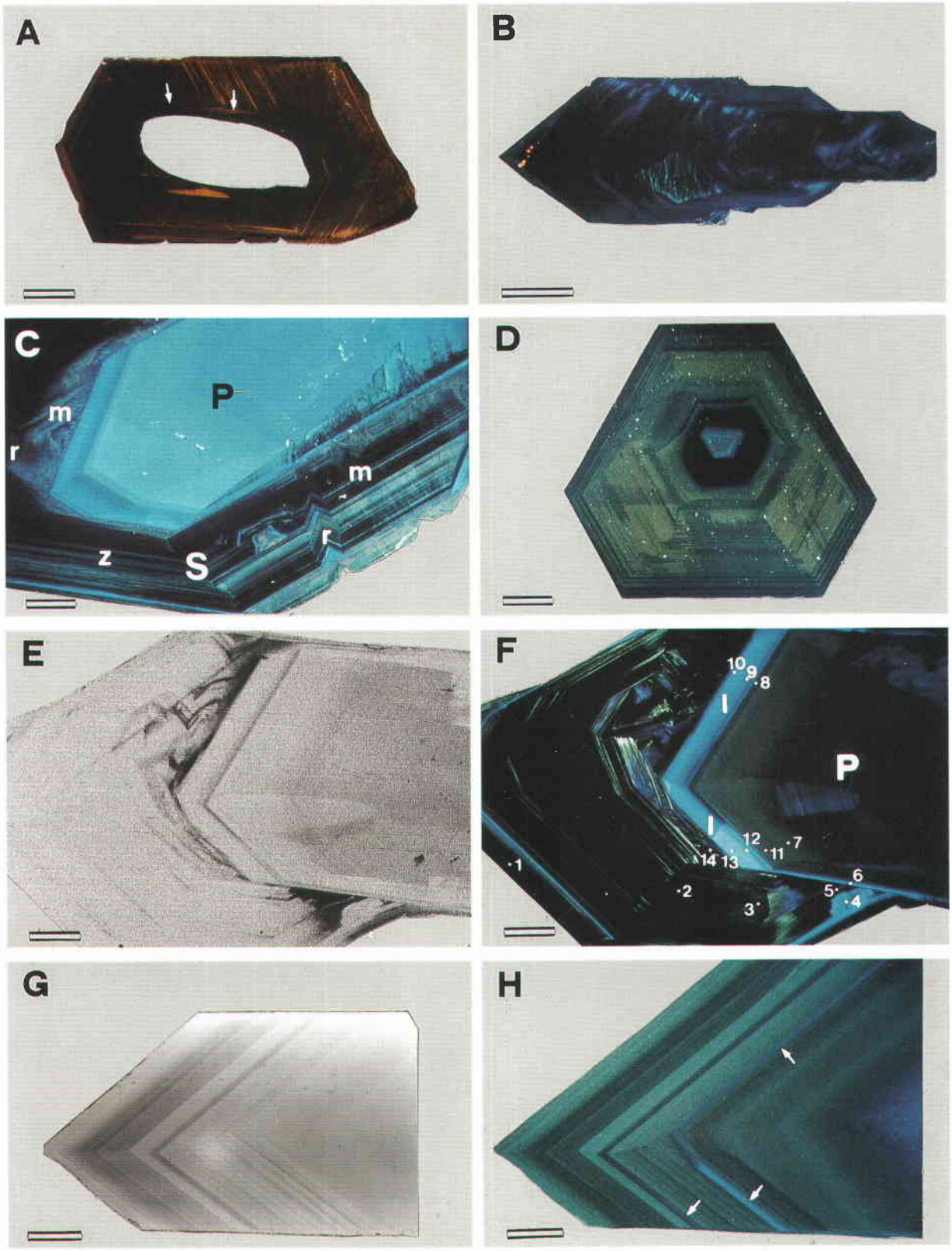
A
B
C
P
m
r
m
r
z
S
D
E
F
10
9
8
l
P
l
12
7
11
14
13
1
2
3
6
5
4
G
H

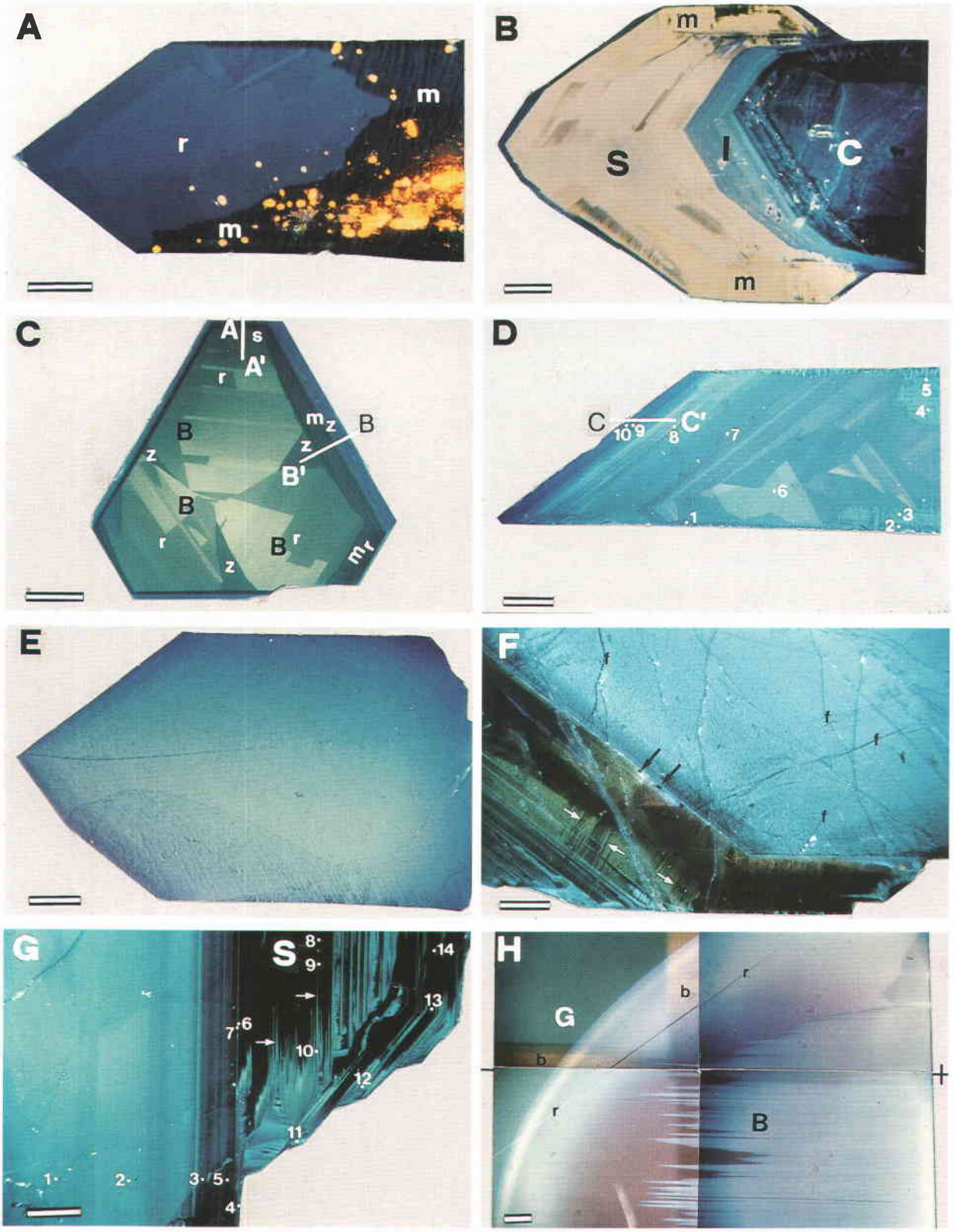
A
m
r
m
B
m
S
I
C
m
C
A
s
A'
r
B
m_z
B
z
z
B'
B
r
B^r
z
m_r
D
C
10
9
8
C'
7
6
5
4
1
2
3
E
F
f
f
f
f
f
G
S
8
9
14
13
7
6
10
12
11
1
2
3
5
4
H
G
b
r
b
r
B

luminescence colors also occur but are less common. Nonluminescent quartz was detected in a few crystals with skeletal growth (Figs. 1A–D, 1F; Kleber, 1970).

With the exception of the brown luminescence, all the above colors faded during electron bombardment. The induced luminescence color is a bluish or reddish brown (Ramseyer et al., 1988; Figs. 3B, 2H).

The spectral response of these various luminescence colors is characterized by broad peaks and combinations of peaks in the violet, blue, green, and yellow-orange region of the visible spectra (Fig. 3). During measurement, continuous change in cathodoluminescence characteristics results from electron bombardment, which leads to a detectable increase in the red region of the spectra. This increase is recognizable in the two spectra on Figure 3 for the blue and blue-green colors. After a few minutes of electron bombardment, the spectral response of these areas of previously blue or blue-green luminescence color (Figs. 3B, 2H) takes the form of a broad peak centered around 650 nm (Ramseyer et al., 1988; Fig. 3B).

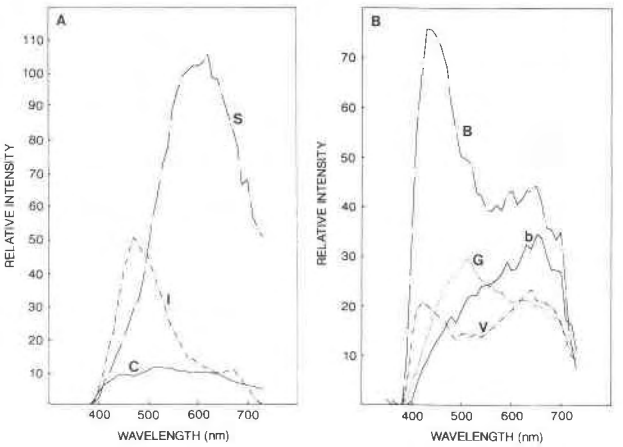

Fig. 3. Spectra of cathodoluminescence colors from quartz crystals. All spectra shown are corrected for instrumental response. (**A**) Luminescence spectra of yellow (S), light blue (I), and dark blue (C) color from the three growth types distinguished in the crystal from Amethystkehle (Fig. 2B). (**B**) Luminescence spectra of blue (B), bottle green (G), brown-violet (V), and artificial brown (b) color from the crystal used in electrodiffusion experiments (Fig. 2H).

The cathodoluminescence pattern in quartz crystals is commonly heterogeneous and related to growth history (Fig. 2). Only ordinary colorless (Bambauer et al., 1961) and smoky quartz exhibit a homogeneous luminescence intensity and color (Figs. 2E, 2F). The cathodoluminescence patterns observed were different for each locality, but crystals taken from the same fissure (i.e., Gigerwald, Figs. 2C, 2D) show similar patterns. Quartz crystals from closely spaced fissures in different rock types (e.g., dolomitic limestone and granite shown by fluid inclusions to have similar thermal histories) also revealed similar cathodoluminescence patterns. The color photographs of Figures 1 and 2 represent the typical cathodoluminescence pattern for a given locality.

Physicochemical growth parameters

The main growth parameters are temperature, pressure, composition, and the concentration of volatiles in the fluids from which quartz precipitated. The effects of each parameter on the cathodoluminescence of quartz were investigated by comparison of the cathodolumi-

←

Fig. 2. Scale bar is 500 μm. (**A**) Fissure quartz from Brunnital, cut parallel to the *c* axis. The part of the crystal luminescing blue represents growth normal to the rhombohedral faces (r), whereas the area with dark blue luminescence (m) contains carbonate luminescing yellow and has growth normal to the prism faces. (**B**) Fissure quartz from Amethystkehle, cut parallel to the *c* axis. In this crystal, the three growth types (continuous slow, cyclic slow, and cyclic rapid) are represented by the core luminescing dark blue (C), the zoned part luminescing lighter blue (I) and the scepter luminescing yellow (S), respectively. Significant growth normal to the prism faces (m) is present in the areas luminescing yellow. (**C**) Fissure quartz from Gigerwald, with cut surface normal to the *c* axis. With luminescence, growth after the positive rhombohedra (r) and the negative rhombohedra (z) are distinguishable, as are both prisms (m_r, m_z), the trapezohedron (s), and Brazil twins (B) in the zone with growth normal to the positive rhombohedra. A-A′ and B-B′ refer to the location of the traverses from Figures 4a and 4b, respectively. (**D**) Fissure quartz from Gigerwald, cut parallel to the *c* axis. The majority of the cyclic slow growth in this crystal was normal to both rhombohedra (r, z) and only a few areas show growth normal to the prisms. The pronounced zonation is typical of this slow cyclic growth. In addition, microprobe analyses show that the outer zone luminescing darker blue contains up to 1410 ppm Al (Fig. 4c; Table 2). The numbers refer to the location of the microprobe analyses from Table 2, and C-C′ to the location of the traverse from Figure 4c. (**E**) Fissure quartz from Grosstal, cut parallel to the *c* axis. The homogeneous cathodoluminescence in this crystal is typical of slow continuous growth. (**F**) Fissure quartz from Val Giuv, cut parallel to the *c* axis. The homogeneous core of the crystal luminescing blue is overprinted by nonluminescent fractures (f). Minute solid impurities on the boundary between the core and the scepter part of the crystal (black arrows) lead to the formation of growth defects visible as nonluminescent thin bands with an orientation approximately normal to the growth faces (white arrows). (**G**) Section of a quartz crystal from Camperio, cut parallel to the *c* axis. Two growth types (e.g., cyclic slow and cyclic rapid) are present in this crystal. In the scepter part (S) of the crystal, the fading of the luminescence along growth layers (white arrows) is directly related to the decrease of Al content from 500 to <50 ppm. The numbers refer to the location of the microprobe analyses from Table 2. (**H**) Section of a quartz crystal from electrodiffusion experiments, cut parallel to the *c* axis. The oblique thin line (r) crossing the whole plate represents growth zonation parallel to a rhombohedral face. The unaltered bottle green luminescing region (G) is characterized by a bottle green luminescence color, whereas the altered region is characterized by streaks of blue luminescence (B) aligned parallel to the *c* axis. The boundary region between the two zones is bell-shaped. The brown luminescence (b) visible in the composite photograph is due to an earlier electron bombardment of this area.

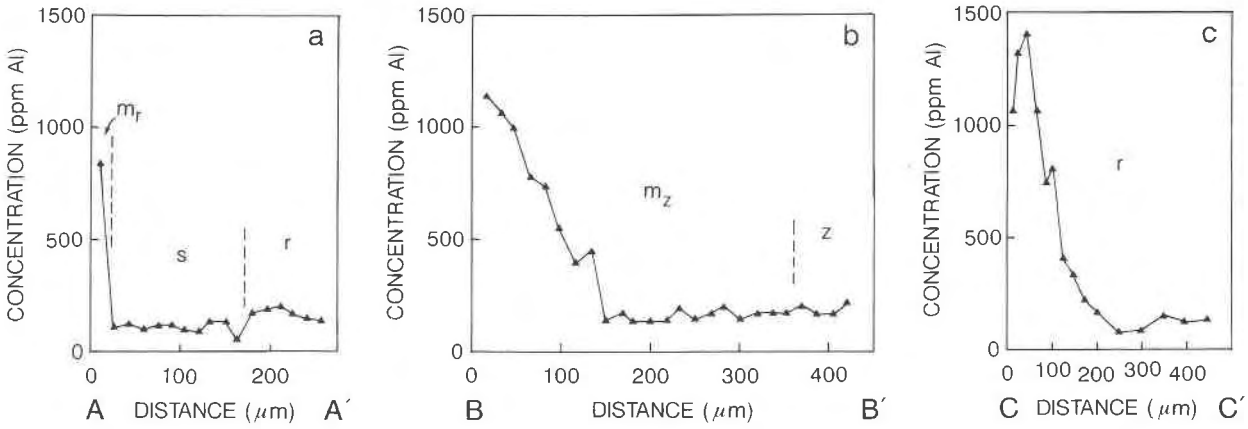

Fig. 4. Electron microprobe traverses across crystals from Gigerwald showing cathodoluminescence zonation. **(a)** Traverse across crystal in Figure 2C (A-A′) over regions with growth normal to the trigonal prism, bipyramid, and positive rhombohedra. **(b)** Traverse across crystal in Figure 2C (B-B′) over regions with growth normal to the trigonal prism and negative rhombohedra. **(c)** Traverse across crystal in Figure 2D (C-C′) over regions with growth normal to the positive rhombohedra.

nescence patterns obtained from crystals grown under different conditions.

Fissure quartz precipitated at similar temperatures and pressures can exhibit variable luminescence intensities. For example, the crystals from Grosstal and the core of the crystals from Val Giuv have a homogeneous blue luminescence (Figs. 2E, 2F), whereas the crystals from Amethystkehle have a dark blue to nonluminescent core (Fig. 2B). In addition, quartz precipitated at different temperatures and pressures (e.g., 120 vs. 200 °C and 40 vs. 150 MPa, Figs. 1C, 1H, 2A, 2C, 2G) can display a similar luminescence color and distribution pattern.

Variations in the amount of CO_2 in the fluid inclusions (e.g., Brunnital: 0.0 mol%; Gigerwald: 3.1 mol%) and in the major volatile species (e.g., the skeletal part of the crystals from Blattenberg: higher hydrocarbons; from Val d'Illiez: CH_4; and from Camperio: CO_2) have no visible effect on the cathodoluminescence color and distribution (Figs. 1B, 1C, 2G).

These examples demonstrate that the temperature and pressure during crystal growth do not influence the cathodoluminescence of α-quartz. In addition, neither a change of the major species (e.g., higher hydrocarbons, CH_4 or CO_2) nor the total amount of volatiles in the fluids have an influence on the cathodoluminescence of α-quartz.

Table 2. Al content of quartz crystals

Number	Val d'Illiez (Fig. 1F) ppm Al	Camperio (Fig. 2G) ppm Al	Gigerwald (Fig. 2D) ppm Al
1	50	60	370
2	60	50	<50
3	70	50	90
4	1940	2750	90
5	280	<50	110
6	1510	3150	130
7	430	1220	100
8	60	<50	130
9	920	<50	1410
10	1960	260	1070
11	280	2100	—
12	990	520	—
13	1370	50	—
14	170	<50	—

Growth dynamics

In addition to temperature, pressure, and volatile content of the fluid, the mode of growth (e.g., continuous, cyclic, slow, or rapid) is another important parameter permitting characterization of these crystals. Three types of crystal growth are distinguishable (Mullis, 1976, 1979, 1980, 1983).

1. Quartz crystals precipitated slowly and continuously from an aqueous chloride solution that was undersaturated in dissolved volatiles. This type of fluid composition is commonly found in fracture systems in tectonically quiescent regions. Quartz crystals from Grosstal (Fig. 2E) and the prismatic cores of the Amethystkehle (Fig. 2B) and Val Giuv (Fig. 2F) crystals are examples of this slow and continuous growth. Homogeneous luminescence is common in this type of quartz.

2. Crystals grown in a slow cyclic manner are characterized by prismatic forms and usually display Dauphinée habits with Brazil twinning and horizontal grooves (Weil, 1930; Friedländer, 1951; Frondel, 1962; Grigoriev, 1965) but without sutures on the prism faces. The outermost zone of the prismatic part of the crystals from Val d'Illiez (Fig. 1C), from Amethystkehle (Fig. 2B) and from Camperio (Fig. 2G), as well as the crystals from Gigerwald and Windgällen (Figs. 1H, 2C), all exhibit finely zoned luminescence consistent with cyclic growth.

3. Crystals characterized by cyclic rapid growth were probably precipitated during boiling (pure H_2O phase) or during fractionation of the fluid-phase into water-rich and volatile-rich components. Phase separations are mostly caused by a sudden pressure drop during fissure enlargements in regions with active tectonism (Mullis, 1987).

The luminescence color and distribution in these rapidly cyclic grown parts of the crystals from Amethystkehle, Val d'Illiez, Camperio, Val Giuv, and Grand Canary are complex, but lack of luminescence in particular growth zones is related to the low Al content of these areas (Figs. 1, 2, 4, Table 2).

The growth dynamics (i.e., continuous vs. cyclic) and the growth speed are thus important controls on the distribution of short-lived cathodoluminescence in α-quartz.

Growth directions

The intensity of short-lived luminescence in quartz crystals from Gigerwald (Fig. 2C, Table 3) decreases from the growth normal to the positive rhombohedra (r) through the negative rhombohedra (z), bipyramid (s), to the trigonal prisms (m_r, m_z). Trends of decreasing intensity are similar both for short-lived blue and induced brown luminescence.

Thus, the intensity of the cathodoluminescence of quartz crystallized in a slow cyclic manner depends primarily on the growth direction.

Density and type of twinning

Crystals showing Brazil twinning (Table 1) may be nonluminescent or else exhibit variable luminescence colors (Fig. 1D). The luminescence pattern generated in the case of Brazil twinning is similar to that produced by γ-irradiation of quartz with a mimetic structure (Friedländer, 1951).

The effect of twinning is also visible on Figure 2C, a quartz crystal from Gigerwald cut perpendicular to the c axis. The difference in luminescence intensity in the same growth sector of the positive rhombohedra (r) and the zigzag boundaries of these sectors are evidence for Brazil twinning (McLaren and Pitkethly, 1982).

Crystal fractures

Large, macro- to microscopic cracks are rare in well-crystallized fissure quartz (Mullis, 1976). If fractures are present, as in the case of the crystal from Val Giuv (Fig. 2E), then the luminescence intensity or color generally differs between the fracture filling and the host quartz.

A good example of submicroscopic lattice defects induced on a discontinuity surface covered with solid particles is visible in the skeletal part of the crystal from Val Giuv (Fig. 2F). The luminescence color in this rapidly grown part of the crystal exhibits defect clusters growing outward similar to the structures observed by Moriya and Ogawa (1978) using light-scattering tomography.

Trace elements

Measurements of Al content were carried out on crystals from Grand Canary, Val d'Illiez, Gigerwald, Grosstal, and Camperio (Figs. 1A, 1F, 2C, 2D, 2E, 2G, 4). The detected Al content varies considerably in most of the crystals exhibiting rapid or discontinuous growth (Table 2). Areas with a high Al content (>1000 ppm Al) always exhibit blue luminescence; but the luminescence intensity of these zones is not always higher than of areas with a lower Al content (e.g., Gigerwald, Camperio).

Table 3. Al concentration in different growth zones of a quartz crystal from Gigerwald (Fig. 2C)

Growth normal to	*n*	ppm Al
Positive rhombohedra (r)	18	181 ± 20
Negative rhombohedra (z)	4	140 ± 20
Bipyramid (s)	12	81 ± 25
Trigonal prism (m_r)	12	120 ± 22
Trigonal prism (m_z)	13	130 ± 21

Analyses of the sample from Gigerwald (Fig. 1D) revealed a significant difference in the Al content between areas with growth normal to the positive rhombohedra (r), the negative rhombohedra (z), the bipyramid (s), and both trigonal prisms (Table 3). The higher Al content in the part with growth normal to the positive rhombohedra corresponds with the higher luminescence intensity in this area. Differences in the Al content of the other areas (i.e., z, m_r, m_z, s) show no relation to the observed luminescence intensity (Table 3, Fig. 1C).

Microprobe measurements in crystals with nonluminescent regions (Grand Canary, Camperio, Val d'Illiez) revealed that short-lived luminescence is absent where the Al content is less than 50 ppm but is generally present in areas with more than 50 ppm Al content (Table 2). A correlation between the Al content and the intensity of the short-lived blue luminescence seems unlikely, since areas with high amounts of Al (>1000 ppm Al) commonly exhibit the same or a darker luminescence than areas of the same crystal with a low (<300 ppm Al) Al content. Charge-balancing cations such as H^+, Li^+, Na^+, or K^+ located in the channels parallel to the *c* axis, may be the causes of the short-lived luminescence in α-quartz.

Artificial and natural γ-irradiation

When the Al-Li pair substitutes for Si and the H content is less than 0.7 ppm, artificial and natural γ-irradiation results in a color change in quartz from transparent to smoky (Bambauer, 1961; Poty, 1969; Nassau, 1978; Fig. 1E). The effect of artificial γ-irradiation on luminescence colors is shown by crystals from Val d'Illiez and Windgällen (Figs. 1E–1H). Slowly grown prismatic parts, areas of the rapidly grown skeletal part, and strongly discolored smoky parts of the artificially irradiated crystals exhibit either no or only low luminescence intensity compared with crystals from the same locality not subjected to artificial γ-irradiation (Fig. 1C). The crystal from Windgällen (Figs. 1G, 1H), which was also artificially irradiated, again shows a lower luminescence intensity in those growth zones with an intense smoky coloration. A decrease in luminescence intensity is also observed in the naturally γ-irradiated quartz (Fig. 2B), with zones of smoky and violet colorations from the Amethystkehle (Nassau, 1978), for which heat treatment resulted in increased intensity of dark blue luminescence in the core.

These examples show that both natural and artificial

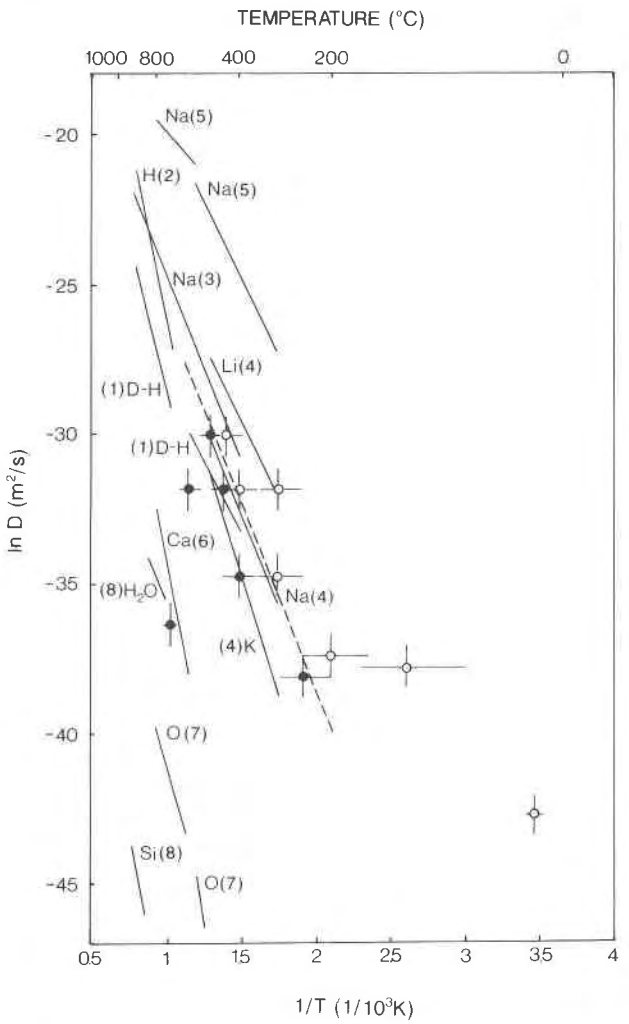

Fig. 5. Arrhenius plot of heat-treated quartz crystals with cut surface normal to the *c* axis. Dots represent conditions where the short-lived luminescence could be restored, whereas circles are for experiments where luminescence was not restored by heat treatment. The dashed boundary between the two areas represents the temperature dependence of the diffusion coefficient causing the short-lived luminescence. Also included are published temperature dependences of the diffusion coefficients parallel to the *c* axis for different ions. (1) D^+-H^+ (Kats et al., 1962); (2) H^+ (Kronenberg et al., 1986); (3) Na^+ (Rybach and Laves, 1967); (4) Li^+, Na^+, K^+ (Verhoogen, 1952); (5) Na^+ (Frischat, 1970a); (6) Ca^{2+} (Frischat, 1970b); (7) O^{2-} (Giletti and Yund, 1984); (8) H_2O, Si^{4+} (Freer, 1981).

γ-irradiation result in local decrease in the intensity of short-lived blue luminescence (although this may be restored through heat treatment). Furthermore, the smoky areas show generally lower luminescence intensities than transparent parts of the same crystal (Figs. 1D–1H). Substitution of Al + Li for Si, which at low H contents causes the smoky coloration, does not itself seem to control the luminescence in α-quartz.

Effect of electrodiffusion

Application of an electric field at elevated temperatures (250–900 °C; Warburg and Tegetmeier, 1888; Verhoogen, 1952; Pfenninger and Laves, 1960; Brunner et al., 1961) is a well-known technique promoting exchange of interstitial cations in quartz. This type of treatment is thus an excellent method for assessing the effects of charged interstitial particles on the color and distribution of the luminescence.

Cathodoluminescence investigation of a quartz crystal used in electrodiffusion experiments (Pfenninger, 1961; Fig. 2H) revealed that the unaltered part of the crystal (on the side of the negative potential) has a homogeneous short-lived bottle-green luminescence color, whereas the remaining altered region (which was located at the positive potential) is characterized by streaks of blue luminescence aligned parallel to the *c* axis. These streaks of linearly polarized blue luminescence originate from the side of the positive potential, where H^+-ions were taken up (Brunner et al., 1961; Pfenninger, 1961). The boundary between the unaltered, bottle-green luminescent zone and the nonluminescent region is gradational and convex in the direction of the position of the negative potential (Fig. 2H). The boundary of the area of stronger luminescence represents the zone of increased cation concentration due to diffusion of cations toward the negative potential (Pfenninger, 1961; Schindler, 1964). Microprobe analyses of each luminescence zone showed no correlation between the Al content, which varies between 90 and 190 ppm Al (mean value 122 ± 35 ppm Al, $n = 10$), and the observed luminescence color. Heating this crystal for one hour at 600 °C generated a more homogeneous short-lived blue to blue-green luminescence color in the area of bottle green luminescence and restored a blue luminescence in the altered regions. These electrodiffusion experiments indicate that the blue, blue-green, and bottle green luminescence is related to the presence of positively charged interstitial cations.

Thermal treatments

Fissure quartz from Grand Canary, Gigerwald, and Grosstal in which luminescence had been destroyed by electron bombardment in the uppermost 5 to 10 μm (at 30 keV, Ramseyer et al., 1989) was thermally treated between 110 and 700 °C for a maximum of 500 h. The original short-lived blue luminescence color and distribution were restored in samples that were heated to high temperatures or kept at moderate temperatures for significantly longer periods of time (e.g., 500 °C for 600 s or 250 °C for 1.8×10^6 s).

Figure 5 is an Arrhenius plot for these data using the measured alteration depth (5–10 μm) to calculate the diffusion coefficient. Time-temperature conditions that regenerated the short-lived luminescence are represented by dots, and conditions with no regeneration of the luminescence are marked as open circles. Thus the first set

of data points (dots) represents time-temperature conditions where the diffusion distance of the species causing the luminescence is equal to or larger than the thickness of the altered zone. The second set of data points (open circles) represents conditions where the diffusion distance is considerably smaller than the alteration depth. The boundary between the two sets of data points represents the time-temperature conditions where the diffusion distance is equal to the alteration depth. These boundary conditions characterize the temperature dependence of the diffusion coefficient for the species causing the short-lived luminescence in α-quartz. A comparison with published data concerning temperature dependences of the diffusion coefficients parallel to the *c* axis for deuterium-hydrogen exchange, H^+, Li^+, Na^+, K^+, Ca^{2+}, Si^{4+}, and O^{2-} ions (Kats et al., 1962; Kronenberg et al., 1986; Rybach and Laves, 1967; Verhoogen, 1952; Frischat, 1970a, 1970b; Giletti and Yund, 1984; Freer, 1981) shows that the temperature dependence of the diffusion coefficient obtained here is similar to data for Na^+, or K^+ ions and the deuterium-hydrogen exchange (Fig. 5). The great difference in the published data for the diffusion of Na^+ ions (see Freer, 1981) and the large experimental error only permit identification of the diffusing species as a single charged cation (Fig. 5).

Discussion

Since the uptake of trace elements into the quartz structure is controlled by crystal-growth parameters and solution chemistry, neither the growth temperature nor the formation pressure should influence the luminescence. Short-lived luminescence in α-quartz is thus controlled by the crystal-growth parameters, growth dynamics (e.g., continuous vs. cyclic and slow vs. rapid), and growth direction. The uptake of Al with a charge-balancing cation as a substitution for Si seems to be the cause of the short-lived blue luminescence colors in α-quartz, since only quartz with more than 50 ppm Al exhibits this type of luminescence.

Observations of luminescence of artificially treated quartz crystals (e.g., electron bombardment, γ-irradiation, electrodiffusion, and thermal treatment) provide additional insights into the nature and origin of the short-lived luminescence in α-quartz. The rapid decrease in luminescence intensity during excitation by highly accelerated electrons, the regeneration of this luminescence through heating, and the redistribution of the luminescence colors after electrodiffusion (Ramseyer et al., 1988) indicate the close relationship between luminescence and the presence of positively charged interstitial ions in channels parallel to the *c* axis. The observations of γ-irradiated crystals and from thermal experiments restrict the possible range of responsible species to the singly charged cations H^+, Na^+, and K^+. In addition, the electrodiffusion experiment reveals that luminescence can result from the uptake of hydrogen (H^+) and the diffusion of cations.

Conclusions

The most important factor influencing the short-lived cathodoluminescence in α-quartz during crystallization is the uptake of charge balancing, singly charged cations associated with the substitution of Si by Al. The concentration and distribution of these trace elements are controlled by (1) the growth dynamics (continuous slow, cyclic slow, or cyclic rapid), (2) the growth direction, and (3) the presence of Brazil twinning. The temperature and pressure conditions of crystal growth do not appear to affect α-quartz luminescence.

After crystallization, natural irradiation by γ-rays or α-particles may modify the luminescence characteristics. In addition, later filled fractures in the crystals may exhibit luminescence colors or intensities that are different from those of the host crystal.

Luminescence in α-quartz is destroyed by electron bombardment, α- and γ-irradiation, and electrodiffusion but is regenerated by heat treatment.

Acknowlegments

This research was funded by the Swiss National Science Foundation (grant no. 2000-5.287), which we gratefully acknowledge. We thank Dr. G.A. Waychunas and Dr. Ian Steele for their helpful comments. Thanks are also due to Dr. J. Zimmermann, Centre de Recherches Pétrographiques et Géochimiques (Nancy, France) for mass spectrometric analyses, to Dr. J. Dubessy, Centre de Recherches sur la Géologie de l'Uranium (Nancy, France) for Raman spectroscopic investigations, to Dr. J. Baumann, Institut für anorganische und physikalische Chemie (Bern) for the analyses of luminescence spectra, and to Dr. T. Armbruster, Dr. M. Frey, Dr. N.H. Platt, and Dr. P. Mozley for reviewing and polishing the English text.

References cited

Bambauer, H.U. (1961) Spurenelementgehalte und γ-Farbzentren in Quarzen aus Zerrklüften der Schweizer Alpen. Schweizerische mineralogische und petrographische Mitteilungen, 41, 335–369.

Bambauer, H.U., Brunner, G.O., and Laves, F. (1961) Beobachtungen über den Lamellenbau an Bergkristallen. Zeitschrift für Kristallographie, 116, 173–181.

Bowers, T.S., and Helgeson, H.C. (1983) Calculation of the thermodynamic and geochemical consequences of nonideal mixing in the system H_2O-CO_2-NaCl on phase relations in geologic systems: Metamorphic equilibria at high pressures and temperatures. American Mineralogist, 68, 1059–1075.

Brunner, G.O., Wondratscheck, H., and Laves, F. (1961) Ultrarot-untersuchungen über den Einbau von H in natürlichem Quarz. Zeitschrift für Elektrochemie, 65, 735–750.

Dhamelincourt, P., Beny, J.M., Dubessy, J., and Poty, B.P. (1979) Analyse d'inclusions fluides à la microsonde MOLE à effet Raman. Bulletin de Minéralogie, 102, 600–610.

Freer, R. (1981) Diffusion in silicate minerals and glasses: A data digest and guide to the literature. Contributions to Mineralogy and Petrology, 76, 440–454.

Friedländer, C. (1951) Untersuchungen über die Eignung alpiner Quarze für piezoelektrische Zwecke. Beiträge zur Geologie der Schweiz, Geotechnische Serie 29.

Frischat, G.H. (1970a) Kationentransport in Quarzkristallen: I. Natriumdiffusion parallel zur c-Achse. Bericht Deutsche Keramische Gesellschaft, 47, 238–243.

——— (1970b) Kationentransport in Quarzkristallen: III. Calciumdiffusion parallel zur c-Achse. Bericht Deutsche Keramische Gesellschaft, 47, 364–368.

Frondel, C. (1962) The system of mineralogy, silica minerals (7th edition), 334 p. Wiley, New York.

Giletti, B.J., and Yund, R.A. (1984) Oxygen diffusion in quartz. Journal of Geophysical Research, 89, 4039–4046.

Goldstein, E. (1907) Über das Auftreten roten Phosphoreszenzlichtes an Geissler' schen Röhren: Bericht der Deutschen Physikalischen Gesellschaft, 598–605.

Grigoriev, D.P. (1965) Ontogeny of minerals. Israel Program of Scientific Translations, p. 250. Jerusalem.

Holloway, J.R. (1981) Compositions and volumes of supercritical fluids in the earth's crust. In L.S. Hollister and M.L. Crawford, Eds., Short course in fluid inclusions. Mineralogical Association of Canada Short Course, 6, 13–38.

Jacobs, G.K., and Kerrik, D.M. (1981) Methane: An equation of state with application to the ternary system H_2O-CO_2-CH_4. Geochimica et Cosmochimica Acta, 45, 607–614.

Kats, A., Haven, Y., and Stevels, J.M. (1962) Hydroxyl groups in α-quartz. Physics and Chemistry of Glasses, 3, 69–75.

Kleber, W. (1970) An introduction to crystallography, 366 p. VEB Verlag Technik, Berlin.

Kronenberg, A.K., Kirby, S.H., Aines, R.D., and Rossman, G.R. (1986) Solubility and diffusional uptake of hydrogen in quartz at high water pressures: Implications for hydrolytic weakening. Journal of Geophysical Research, 91, 12723–12744.

Long, J.V.P., and Agrell, S.O. (1965) The cathodoluminescence of minerals in thin section. Mineralogical Magazine, 34, 318–326.

Matter, A., and Ramseyer, K. (1985) Cathodoluminescence microscopy as a tool for provenance studies of sandstones. NATO ASI Series, 148, 191–211.

McLaren, A.C., and Pitkethly, D.R. (1982) The twinning microstructure and growth of amethyst quartz. Physics and Chemistry of Minerals, 8, 128–135.

Moriya, K., and Ogawa, T. (1978) Observation of growth defects in synthetic quartz crystals by light-scattering tomography. Journal of Crystal Growth, 44, 53–60.

Mullis, J. (1975) Growth conditions of quartz crystals from Val d'Illiez (Valais, Switzerland). Schweizerische mineralogische und petrographische Mitteilungen, 55, 419–430.

——— (1976) Das Wachstumsmilieu der Quarzkristalle im Val d'Illiez. Schweizerische mineralogische und petrographische Mitteilungen, 56, 219–268.

——— (1979) The system methane-water as a geologic thermometer and barometer from the external part of the Central Alps. Bulletin de Minéralogie, 102, 526–536.

——— (1980) Quarzkristalle aus den Maderanertal. Lapis, 5, 19–21.

——— (1982) Sternquarz. Schweizer Strahler, 6, 125–140.

——— (1983) Einschlüsse in Quarzkristallen der Schweizer Alpen und ihre mineralogisch-geologische Bedeutung. Bulletin de la Societé fribourgeoise des Sciences naturelles, 72, 5–19.

——— (1987) Fluid inclusion studies during very low-grade metamorphism. In M. Frey, Ed., Low temperature metamorphism, p. 162–199. Backie, Glasgow.

Mullis, J., and Sigl, F. (1982) Die Entstehungsgeschichte von Opal, Chalcedon und Quarz von Gran Canaria. Schweizer Strahler, 6, 155–176.

Nassau, K. (1978) The origins of color in minerals. American Mineralogist, 63, 219–229.

Pfenninger, H.H. (1961) Diffusion von Kationen und Abscheidung von Metallen in Quarz unter elektrischer Feldeinwirkung. Ph.D. thesis, University of Zürich, 130 p.

Pfenninger, H.H., and Laves, F. (1960) Kationenwanderung und Farbzentrenbildung bei der Elektrolyse von Quarzplatten senkrecht zur optischen Achse. Naturwissenschaften, 47, 276.

Potter, R.W., and Brown, D.L. (1977) The volumetric properties of aqueous sodium chloride solutions from 0° to 500°C and pressures up to 2000 bars based on a regression of available data in the literature. U.S. Geological Survey Open-file Report 75-636, 31 p.

Poty, B.P. (1969) La croissance des cristaux de quartz dans les filons sur l'example du filon de La Gardette (Bourg d'Oisans) et des filons du massif du Mont Blanc. Thèse Université de Nancy, Science de la Terre, Mémoir 17.

Poty, B.P., Leroy, J., and Jachimowicz, L. (1976) Un nouvel appareil pour la mesure des températures sous la microscope: l'installation de microthermométrie Chaixmeca. Bulletin de Minéralogie, 99, 182–186.

Ramboz, C., Schnapper, D., and Dubessy, J. (1985) The P-V-T-X-fO_2 evolution of H_2O-CO_2-CH_4 bearing fluid in a wolframite vein: Reconstruction from fluid inclusion studies. Geochimica et Cosmochimica Acta, 49, 205–219.

Ramseyer, K., Baumann, J., Matter, A., and Mullis, J. (1988) Cathodoluminescence colours of α-quartz. Mineralogical Magazine, 52, 669–677.

Ramseyer, K., Fischer, J., Matter, A., Eberhardt, P., and Geiss, J. (1989) A cathodoluminescence microscope for low intensity luminescence. Journal of Sedimentary Petrology, 59, 619–622.

Roedder, E. (1984) Fluid inclusions. Mineralogical Society of America Reviews in Mineralogy, 12, 646 p.

Rybach, L., and Laves, F. (1967) Sodium diffusion experiments in quartz crystals. Geochimica et Cosmochimica Acta, 31, 539–546.

Schindler, P. (1964) Untersuchungen eines paramagnetischen Defektes in Quarz. Ph.D. thesis, University of Zürich, 53 p.

Sippel, R.F. (1965) Simple device for luminescence petrography. Review of Scientific Instruments, 36, 1556–1558.

——— (1968) Sandstone petrology, evidence from luminescence microscopy. Journal of Sedimentary Petrology, 38, 530–554.

Smith, J.V., and Stenstrom, R.C. (1965) Electron-excited luminescence as a petrologic tool. Journal of Geology, 73, 627–635.

Sprunt, E.S., Dengler, L.A., and Sloan, D. (1978) Effects of metamorphism on quartz cathodoluminescence. Geology, 6, 305–308.

Verhoogen, J. (1952) Ionic diffusion and electrical conductivity in quartz. American Mineralogist, 37, 637–655.

Warburg, E., and Tegetmeier, F. (1888) Über die electrolytische Leitung des Bergkrystalls. Annalen der Physik und Chemie, 35, 455–467.

Weil, R. (1930) Observations sur le quartz. Comptes rendus hebdomadaires des seances de l'Academie des sciences Paris sciences naturelles, 191, 270–272, 380–382, 935–937.

Zinkernagel, U. (1978) Cathodoluminescence of quartz and its application to sandstone petrology. Contributions to Sedimentology, 8, 1–69.

Manuscript received December 14, 1988
Manuscript accepted May 14, 1990